Journal of Nuclear Medicine, published on July 31, 2014 as doi:10.2967/jnumed.114.138594

A Randomized Trial on the Optimization of ^{18}F-FDG Myocardial Uptake Suppression: Implications for Vulnerable Coronary Plaque Imaging

Fabian Demeure[1], François-Xavier Hanin[2], Anne Bol[2], Marie-Françoise Vincent[3], Anne-Catherine Pouleur[1], Bernhard Gerber[1], Agnès Pasquet[1], François Jamar[2], Jean-Louis J. Vanoverschelde[1], and David Vancraeynest[1]

[1]From the Pôle de Recherche Cardiovasculaire (CARD), Institut de Recherche Expérimentale et Clinique (IREC), Université Catholique de Louvain, Brussels, Belgium; [2]From the Pôle d'imagerie Médicale, Radiothérapie et Oncologie (MIRO), Institut de Recherche Expérimentale et Clinique (IREC), Université Catholique de Louvain, Brussels, Belgium; and [3]From the Laboratoire des Maladies Métaboliques et Centre de Dépistage Néonatal, Cliniques Universitaires St-Luc, Université Catholique de Louvain, Brussels, Belgium

^{18}F-FDG PET/CT can be used to detect arterial atherosclerotic plaque inflammation. However, avid myocardial glucose uptake may preclude its use for visualizing coronary plaques. Fatty acid loading or calcium channel blockers could decrease myocardial ^{18}F-FDG uptake, thus assisting coronary plaque inflammation identification. The present prospective randomized trial compared the efficacies of different interventions for suppressing myocardial ^{18}F-FDG uptake. We also investigated whether circulating free fatty acid (cFFA) levels predicted the magnitude of myocardial ^{18}F-FDG uptake. **Methods:** Thirty-six volunteers ate a high-fat low-carbohydrate meal, followed by a 12-h fasting period. They were then randomized to 1 of 4 intervention groups. Group 1 received no additional preparation and served as a reference. Groups 2 and 3, respectively, received a commercial high-fat solution containing 43.8 g of lipids or 50 mL of olive oil 1 h before ^{18}F-FDG injection to evaluate the impact of fatty acid loading on myocardial ^{18}F-FDG uptake. Group 4 received verapamil to evaluate the effect of calcium channel blockers. Cardiac PET/CT was performed after administration of 370 MBq of ^{18}F-FDG. Myocardial uptake suppression was assessed using a qualitative visual scale and by measuring the myocardial maximum standardized uptake value (SUV_{max}). Insulin, glucose, and cFFA were serially measured. **Results:** The qualitative visual scale showed good myocardial ^{18}F-FDG uptake suppression in 8 of 9, 5 of 9, 4 of 9, and 8 of 9 subjects of groups 1, 2, 3, and 4, respectively ($P = 0.09$). SUV_{max} did not significantly differ between groups ($P = 0.17$). Interestingly, cFFA levels were higher in volunteers with good suppression (0.80 ± 0.31 mmol/L) than in those with poor suppression (0.53 ± 0.15 mmol/L; $P = 0.011$). We found an inverse correlation between cFFA level (measured at ^{18}F-FDG injection) and the SUV_{max} ($R = 0.61$). Receiver-operating-characteristic curve analysis identified 0.65 mmol/L cFFA as the best cutoff value to predict adequate ^{18}F-FDG uptake suppression (positive predictive value, 89%). **Conclusion:** A high-fat low-carbohydrate meal followed by a 12-h fasting period effectively suppressed myocardial ^{18}F-FDG uptake in most subjects. Neither complementary fatty acid loading nor verapamil administered 1 h before ^{18}F-FDG injection conferred any additional benefit. Myocardial ^{18}F-FDG uptake was inversely correlated with cFFA level, representing an interesting way to predict myocardial ^{18}F-FDG uptake suppression.

Received Feb. 4, 2014; revision accepted Jun. 30, 2014.

For correspondence or reprints contact: David Vancraeynest, Division of Cardiology, Cliniques Universitaires St-Luc, Avenue Hippocrate, 10-2881, B-1200 Brussels, Belgium.

E-mail: David.Vancraeynest@uclouvain.be

Published online ••••••••••••.

Key Words: free fatty acids; ^{18}F-FDG PET/CT; calcium channel blocker; inflammation; vulnerable coronary plaque

J Nucl Med 2014; 55:1–7
DOI: 10.2967/jnumed.114.138594

Cardiovascular diseases are still a leading cause of mortality in western countries (*1*). The high mortality rate of cardiovascular diseases results from arterial thrombosis, which is often triggered by a ruptured plaque. Rupture-prone plaques—also called vulnerable plaques—exhibit typical features, among which inflammation is a key factor (*2–4*). Metabolically active cells, such as activated macrophages, take in and progressively accumulate ^{18}F-FDG, which can then be imaged and quantified with PET. ^{18}F-FDG is a well-validated tracer for imaging plaque inflammation in large arteries and aorta (*5,6*). However, coronary artery imaging is more challenging, mainly because of intense tracer uptake in adjacent myocardium.

The quantity and quality of substrate supply to the heart are determined by the dietary state. Long-chain free fatty acids (FFAs) are the major substrates for the heart. Under fasting conditions, FFAs are released from the adipose tissue, enter the circulation, and are taken up by cardiac cells. FFAs inhibit glycolysis, rerouting glucose toward glycogen synthesis. On the other hand, glycogen phosphorylase is the main regulator of glycogenolysis and is activated by phosphorylation, either by cyclic adenosine monophosphate–dependent protein kinase or by Ca^{2+}-activated phosphorylase kinase (*7*). Intracellular calcium acts as a stimulus for cardiac glucose uptake. Accordingly, it has been demonstrated that high-fat low-carbohydrate (HFLC) dietary preparations can significantly reduce myocardial ^{18}F-FDG uptake in oncologic patients (*8–10*), and calcium channel blockers (CCBs) may help to reduce myocardial ^{18}F-FDG uptake in a murine model (*11*). However, randomized trials evaluating the impact of these interventions on reducing ^{18}F-FDG uptake are lacking.

Also the optimal time point to perform PET acquisition after ^{18}F-FDG injection remains poorly known. Preliminary studies evaluating ^{18}F-FDG PET/CT as a method for coronary plaque inflammation imaging have performed PET at 3 h after ^{18}F-FDG injection (*12–14*). On the other hand, studies evaluating the impact of dietary regimen on the quality of ^{18}F-FDG uptake suppression

RGB

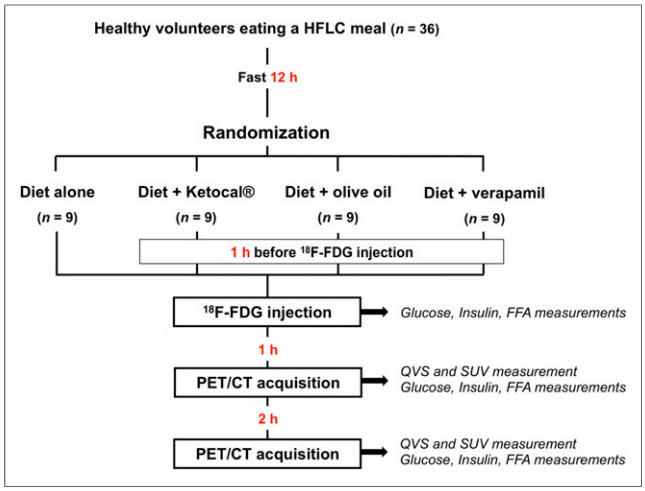

FIGURE 1. Study protocol.

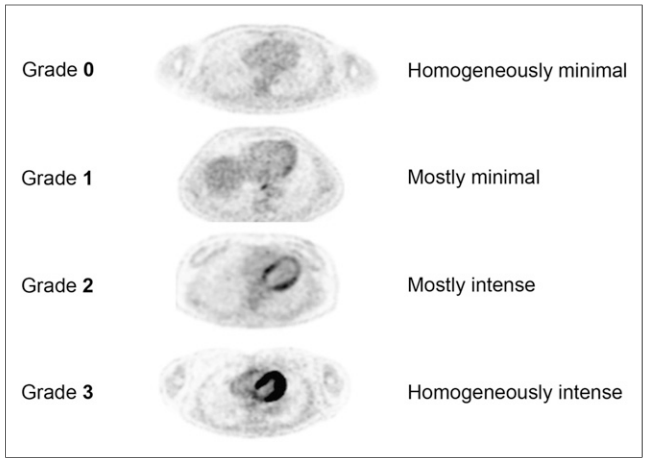

FIGURE 2. QVS assessing myocardial ^{18}F-FDG uptake.

have performed PET at 1 h after ^{18}F-FDG injection (*8,10*). No data are available regarding the impact of the dietary regimen on ^{18}F-FDG uptake at different time intervals.

The present prospective randomized study evaluated the impacts of different interventions—including complementary FFA loading and CCBs—on unwanted myocardial ^{18}F-FDG uptake. We also sought to determine whether measuring insulin, glucose, or circulating FFA (cFFA) level could predict the amplitude of ^{18}F-FDG uptake suppression. Finally, to clarify the most appropriate time point for imaging coronary plaque inflammation, we evaluated the impact of different interventions on the myocardial ^{18}F-FDG signal at different time points.

MATERIALS AND METHODS

Study Population and Intervention Assignment

Thirty-six healthy volunteers were recruited among the paramedical staff of the hospital and were paid for their participation. They were instructed to eat an HFLC meal based on a list of appropriate and inappropriate food items (established by the dietetic department) and then to fast (water permitted) for 12 ± 1 h. A preimaging interview was systematically conducted to precisely check the composition of the meal ingested the evening before. The volunteers were then randomly assigned, by drawing lots, to 1 of the following 4 pre–^{18}F-FDG PET/CT intervention plans (9 volunteers in each group). Group 1 did not receive any additional preparation to evaluate the effect of HFLC diet alone and served as a reference. Group 2 received a 250-mL liquid mixture containing a commercial high-fat solution (KetoCal; SHS International Ltd.)—comprising 43.8 g of fat (78% unsaturated), 1.8 g of carbohydrate, and 9.15 g of protein—at 60 min before ^{18}F-FDG injection to evaluate the effect of complementary fatty acid loading on ^{18}F-FDG uptake. Group 3 received 50 mL of olive oil (46 g of fat, without carbohydrate or protein) at 60 min before ^{18}F-FDG injection to evaluate the effect of another form of complementary fatty acid loading on ^{18}F-FDG uptake. Group 4 received 120 mg of verapamil (orally) at 60 min before ^{18}F-FDG injection to evaluate the effect of CCBs on ^{18}F-FDG uptake (Fig. 1). The volunteers were instructed to [**Fig. 1**] avoid exercise, alcohol, benzodiazepine, and caffeine for at least 24 h before the injection. Pregnancy was an exclusion criterion, and all female volunteers underwent urine pregnancy testing. All volunteers gave their written informed consent, and the study protocol was approved by the ethical committee of our institution.

^{18}F-FDG PET/CT Imaging Protocol

Imaging was performed at 60 and 180 min after intravenous administration of 370 MBq of ^{18}F-FDG to evaluate the impact of the

TABLE 1
Baseline Characteristics of Volunteers

Characteristic	Group 1, diet alone (*n* = 9)	Group 2, Ketocal (*n* = 9)	Group 3, olive oil (*n* = 9)	Group 4, verapamil (*n* = 9)	*P*
Age (y)	26 ± 4	24 ± 3	26 ± 5	27 ± 8	0.78
Sex					0.71
Male	6	7	5	7	
Female	3	2	4	2	
Body mass index (kg/m^2)	22 ± 2	24 ± 2	24 ± 4	22 ± 2	0.32
Systolic blood pressure (mm Hg)	124 ± 10	128 ± 9	126 ± 15	123 ± 15	0.87
Diastolic blood pressure (mm Hg)	75 ± 10	75 ± 10	72 ± 14	78 ± 12	0.86
Heart rate (bpm)	70 ± 14	83 ± 10	84 ± 15	75 ± 8	0.06
Glucose (mg/dL)	87 ± 8	91 ± 8	88 ± 10	90 ± 11	0.72

Values are expressed as mean ± SD or as number.
Bpm = beats per minute.

jnm138594-pm ■ 7/31/14

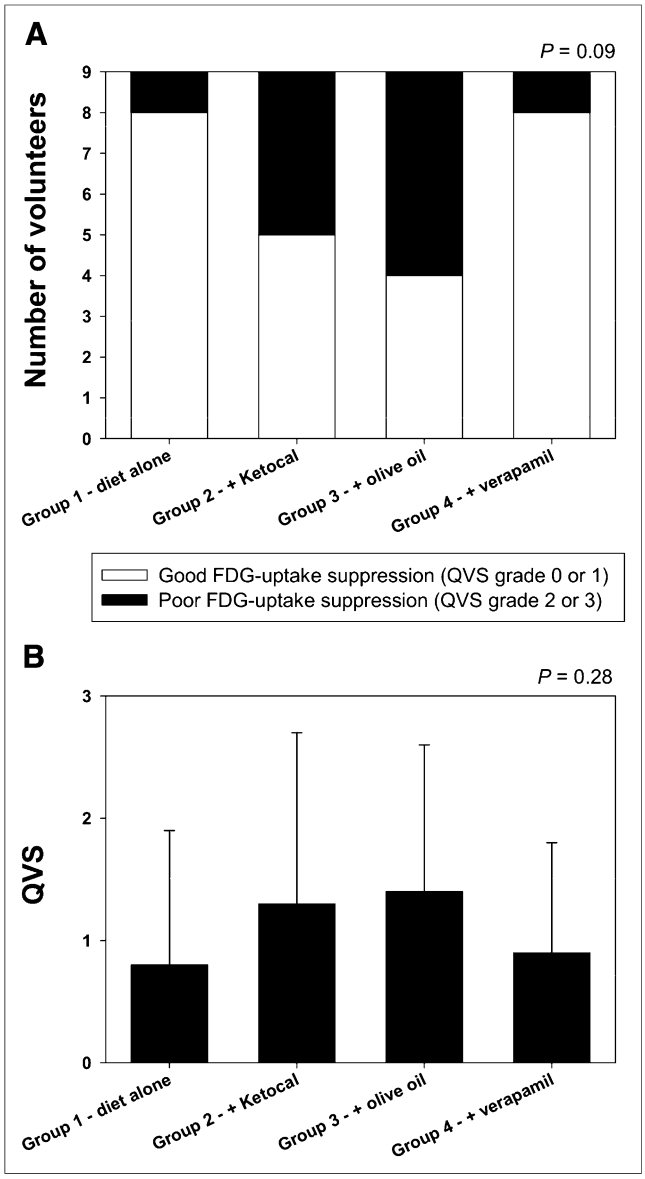

FIGURE 3. Box plots showing number of volunteers with good (QVS grades 0 or 1) or poor (QVS grades 2 or 3) myocardial ^{18}F-FDG uptake suppression in each group ($P = 0.09$) (A) and mean QVS grade in each group at 60 min ($P = 0.28$) (B).

intervention on myocardial uptake at 2 different time intervals. Images were acquired using a Gemini PET/CT system (Philips Healthcare). The used equipment complied with the European Association of Nuclear Medicine Research Ltd. accreditation ^{18}F-FDG PET/CT requirements for clinical research (*15*). The volunteers breathed normally while CT imaging was performed with a 16-slice multidetector scanner (adaptive dose in Z-DOM mode; voltage, 120 kV; rotation, 500 ms; pitch, 0.813). PET images (voxel size, 4 × 4 × 4 mm) were obtained in 3-dimensional mode from the neck to the liver, with 5 min per bed position, and were iteratively reconstructed (3-dimensional line of response time-of-flight algorithm; Philips) using CT-based attenuation correction and random and scatter corrections. The volunteers were kept in a quiet environment before and between the 2 imaging time points. The effective radiation dose from ^{18}F-FDG was estimated at 7.1 ± 0.2 mSv, using ICRP publication 106 (0.019 mSv/MBq conversion factor) (*16*). The effective radiation dose from CT was 2.1 ± 1.0 mSv per procedure.

Image Analysis

Myocardial ^{18}F-FDG uptake was assessed on 60- and 180-min images using a qualitative visual scale (QVS) based on the visual uptake categoric scale proposed by Williams and Kolodny (*10*). The qualitative visual estimation of ^{18}F-FDG myocardial uptake was graded as follows: 0, homogeneously minimal; 1, mostly minimal or mild uptake; 2, mostly intense or moderate uptake; or 3, homogeneously intense (Fig. 2). QVS grades of 0 and 1 were considered good suppression, [**Fig. 2**] whereas QVS grades of 2 and 3 were considered poor suppression. To evaluate the interobserver reliability of the visual grading, images were graded by 2 independent investigators who were masked to the group assignment of each volunteer.

We also quantitatively assessed the myocardial ^{18}F-FDG uptake by measuring the maximum standardized uptake value (SUV_{max}). On the basis of anatomic boundaries defined by CT, a region of interest was drawn around the left ventricle in the axial view at the level of the anterolateral papillary muscle, which was included in the analysis. To obtain a background value for ^{18}F-FDG uptake, 6 regions of interest of 1 cm^2 each were drawn within the left atrium, and the mean SUV was measured and averaged. Subsequently, for each volunteer, the target-to-background ratio (TBR) was calculated as the myocardial SUV_{max} divided by atrial blood mean SUV.

Blood Analysis

Blood samples were collected at ^{18}F-FDG injection and at both imaging times (60 and 180 min after ^{18}F-FDG injection) for measurement of glucose, insulin, and cFFA levels (Fig. 1). cFFA was measured using an enzymatic colorimetric method (NEFA-HR(2) assay; Wako Life Sciences, Inc.). All measurements were performed in duplicate.

Statistical Analysis

Group comparisons of categoric variables were made using the Pearson χ^2 test. Continuous variables were expressed as mean ± SD. Continuous variables were compared between 2 groups using the Student *t* test and were compared among all groups using ANOVA (Kruskal–Wallis). Individual comparisons between groups were evaluated post hoc using the Mann–Whitney test. We categorized the volunteers into tertiles according to cFFA level and applied a trend test across ordered groups to assess the relationship between cFFA level and SUV_{max}. We performed a nonlinear regression between the values of SUV_{max} measured at 60 min and the cFFA level obtained at the time of injection. κ statistics were used to determine the levels of agreement between the visual grading scores of the 2 readers. For all analyses, differences with a *P* value of less than 0.05 were considered significant. Receiver-operating-characteristic curve analysis was used to identify the best cFFA level cutoff value for predicting myocardial ^{18}F-FDG uptake suppression. All statistical analyses were performed using SPSS statistical software (version 15.0; SPSS).

RESULTS

There were no significant between-group differences in age, body mass index, blood pressure, heart rate, and pre–^{18}F-FDG-injection glucose level (Table 1). [**Table 1**]

Impact of FFA Loading and CCB on Myocardial ^{18}F-FDG Uptake Suppression

QVS grades of 0 or 1, indicating good myocardial uptake suppression, were observed in 8 of 9 volunteers in group 1, 5 of 9 volunteers in group 2, 4 of 9 volunteers in group 3, and 8 of 9 volunteers in group 4 (Fig. 3A; $P = 0.09$). The mean QVS grade [**Fig. 3**] did not significantly differ between groups (Fig. 3B; $P = 0.28$). The quantitative analysis showed that at 60 min after ^{18}F-FDG administration, the myocardial SUV_{max} did not significantly differ between groups (group 1, 2.3 ± 0.8; group 2, 4.6 ± 3.3; group 3,

jnm138594-pm ■ 7/31/14

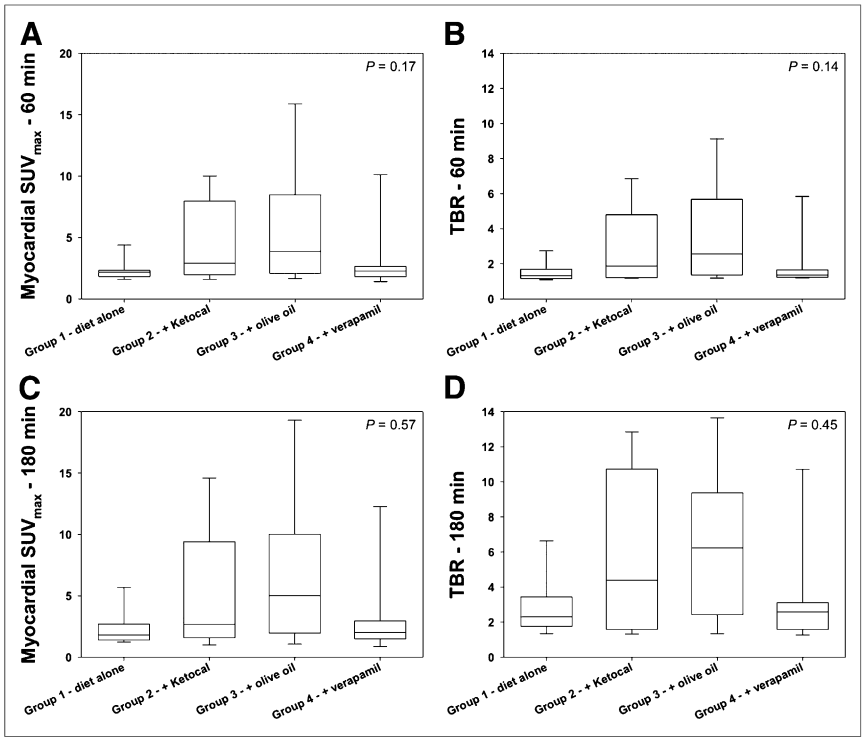

FIGURE 4. Box plots showing comparisons among study groups of myocardial SUV_{max} measured 60 min after ^{18}F-FDG injection ($P = 0.17$) (A), TBRs measured 60 min after ^{18}F-FDG injection ($P = 0.14$) (B), myocardial SUV_{max} measured 180 min after ^{18}F-FDG injection ($P = 0.57$) (C), and TBRs measured 180 min after ^{18}F-FDG injection ($P = 0.45$) (D).

[Fig. 4] 5.5 ± 5.1; and group 4, 3.0 ± 2.7; Fig. 4A; $P = 0.17$). Similar results were obtained at 60 min for the TBR values (group 1, 1.50 ± 0.52; group 2, 2.93 ± 2.12; group 3, 3.53 ± 2.89; and group 4, 1.86 ± 1.50; Fig. 4B; $P = 0.14$).

Influence of Time-Point Imaging

Imaging was performed at 60 and 180 min after ^{18}F-FDG injection, and the acquired images were compared. At the 180-min post–^{18}F-FDG injection imaging, myocardial SUV_{max} did not significantly differ between groups (group 1, 2.3 ± 1.4; group 2, 5.3 ± 4.9; group 3, 6.8 ± 6.9; and group 4, 3.2 ± 3.5; Fig. 4C; $P = 0.57$). The myocardial SUV_{max} remained stable within each group between the 2 time points. On the other hand, because the left atrial SUV_{max} decreased in the same time, the TBR values increased significantly over time in each group ($P = 0.009$, 0.015, 0.011, and 0.024 for groups 1, 2, 3, and 4, respectively). However, at 180 min, the TBR values did not significantly differ between groups (group 1, 2.79 ± 1.64; group 2, 5.63 ± 4.69; group 3, 6.37 ± 4.93; and group 4, 3.21 ± 2.90; Fig. 4D; $P = 0.45$). Similarly, because the visual analysis accounted for the background activity and because that background activity decreased between the time points, we found that 5 volunteers who had a good myocardial extinction (QVS grade 1) at 60 min were reclassified as QVS-2 after 180 min.

Blood Analysis

At ^{18}F-FDG injection, the glucose, insulin, and FFA levels were similar among the 4 study groups ($P = 0.78$, 0.12, and 0.26, respectively). As expected, the glucose and insulin levels decreased after 60 and 180 min, whereas the FFA level slightly increased over time. Interestingly, volunteers with good (QVS grades 0 or 1) versus poor (QVS grades 2 or 3) myocardial ^{18}F-FDG uptake suppression did not exhibit significantly different glucose ($P = 0.97$; Fig. 5A) and insulin [Fig. 5] ($P = 0.50$; Fig. 5B) levels; however, volunteers with good myocardial ^{18}F-FDG uptake suppression showed significantly higher FFA levels than those with poor myocardial ^{18}F-FDG uptake suppression (0.80 ± 0.31 vs. 0.53 ± 0.15 mmol/L, respectively; $P = 0.011$; Fig. 5C).

Correlation with Blood Parameters

We observed a linear trend toward greater suppression in myocardial ^{18}F-FDG uptake measured at 60 min after ^{18}F-FDG injection, with the highest cFFA levels obtained at the time of ^{18}F-FDG injection (P for trend < 0.001; Fig. 6). When assessed continuously, [Fig. 6] the cFFA level was significantly related to the suppression of myocardial ^{18}F-FDG uptake ($r = 0.61$; $P < 0.001$). However, myocardial ^{18}F-FDG uptake suppression was not correlated with glucose ($r = 0.10$; $P = 0.54$) or insulin level ($r = 0.08$; $P = 0.65$). Receiver-operating-characteristic analysis demonstrated that a cFFA concentration of greater than 0.65 mmol/L measured at the time of ^{18}F-FDG injection had 68% sensitivity, 82% specificity, and 89% positive predictive value to predict good ^{18}F-FDG uptake suppression (area under the curve, 0.80; Fig. 7). [Fig. 7]

Interobserver Variability

We found a high κ statistic for interobserver variability of the visual assessment of ^{18}F-FDG uptake ($\kappa = 0.8$).

DISCUSSION

This prospective randomized study demonstrates that an HFLC diet administered the evening before ^{18}F-FDG PET/CT followed by 12 h of fasting is an effective method to obtain good myocardial ^{18}F-FDG uptake suppression. Furthermore, our data showed no additional benefit of administering complementary fatty acid loading or CCB 1 h before ^{18}F-FDG injection. One salient finding of this study is the observation that ^{18}F-FDG uptake was inversely correlated with cFFA levels, which could be used to accurately predict the amplitude of myocardial ^{18}F-FDG uptake suppression. This method should allow the avoidance of unnecessary ^{18}F-FDG injection in some patients who are not properly prepared. Finally, our study showed that SUV_{max} remained stable over time, permitting the imaging of coronary inflammation at either 60 or 180 min after ^{18}F-FDG injection.

Although several interesting tracers are being evaluated for vulnerable plaque imaging (*17,18*), ^{18}F-FDG PET/CT is currently the most well-evaluated and available tracer for plaque inflammation imaging. In humans with carotid atherosclerosis, areas of high ^{18}F-FDG uptake colocalize with areas of macrophage accumulation (*6,19,20*) and can predict subsequent acute ischemic events (*21,22*). Avid ^{18}F-FDG uptake by the myocardium represents the main challenge to overcome before ^{18}F-FDG PET/CT can be used for imaging coronary plaque inflammation. The present study provides important information regarding how to prepare patients before performing coronary ^{18}F-FDG PET/CT, and our

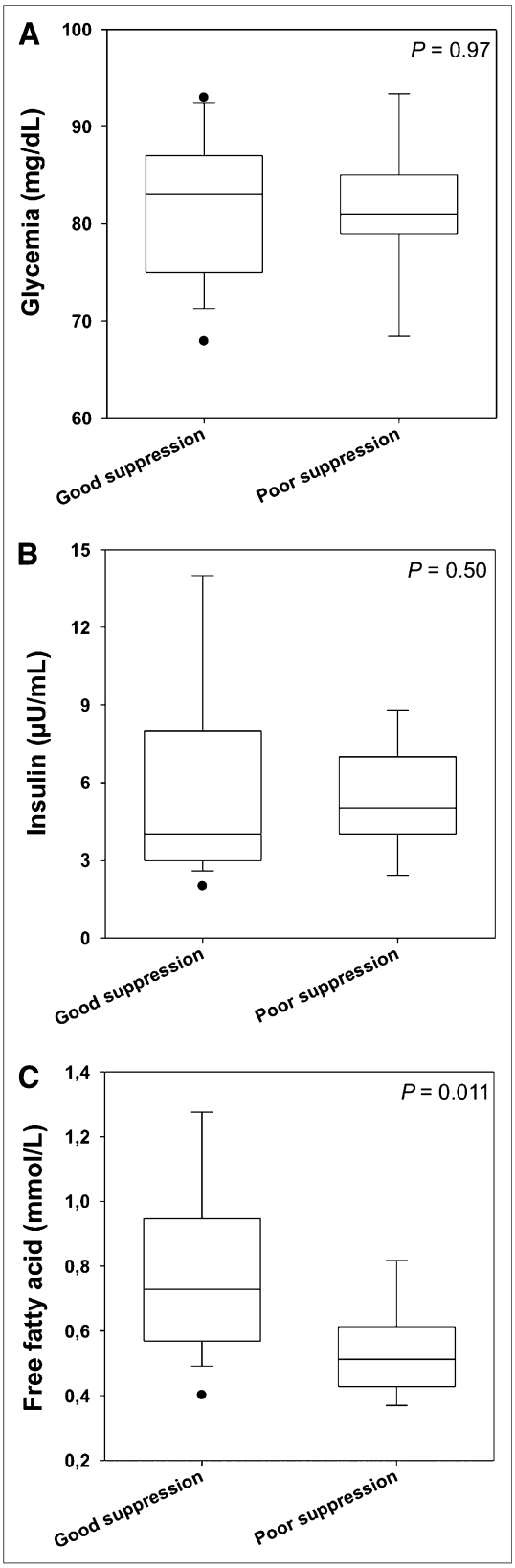

FIGURE 5. Box plots showing comparisons between volunteers with good vs. poor myocardial ^{18}F-FDG uptake suppression (at 60 min) with regard to glucose (P = 0.97) (A), insulin (P = 0.50) (B), and FFA level (P = 0.011) (C) measured at time of ^{18}F-FDG injection.

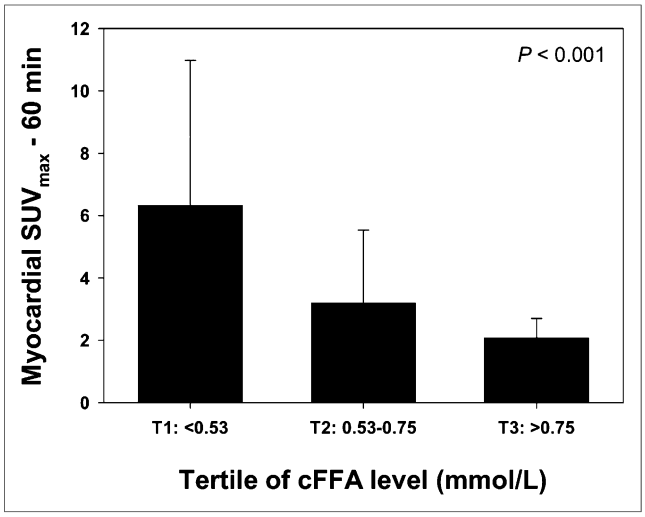

FIGURE 6. Box plot showing relationship between myocardial SUV_{max} measured 60 min after ^{18}F-FDG injection and tertiles of cFFA level obtained at ^{18}F-FDG injection (P for trend < 0.001). T1 = tertile 1; T2 = tertile 2; T3 = tertile 3.

findings are in agreement with previously published retrospective and nonrandomized data (*8,10,13,23*). In the fasted state, such as that imposed on our volunteers, the cFFA level is high and the oxidative metabolism is preferentially dependent on high rates of fatty acid uptake. Furthermore, the volunteers were asked to eat an HFLC meal the evening before imaging, thus inducing an increase in blood triglycerides during postprandial lipemia. Triglycerides are converted by the lipoprotein lipase to FFAs, which then enter fatty acid oxidation pathways. This metabolic pathway explains a very low SUV_{max} of our group 1 volunteers (2.3 ± 0.8), which was significantly lower than the SUV_{max} that we measured in conventionally prepared (6-h fasting period) 100 consecutive oncologic patients who underwent ^{18}F-FDG PET/CT at our institution (SUV_{max}, 6.8 ± 4.8; P = 0.04; data not shown).

We further found that complementary fatty acid loading (>40 g of fat administered 1 h before imaging in groups 2 and 3) provided no additional benefit, compared with the fasted volunteers of group 1. There are several potential reasons for this. First, volunteers of all groups had an HFLC meal the evening before imaging, thus inducing an increase in blood triglycerides. Second, the time between the additional fatty loading and ^{18}F-FDG injection may have been too brief to further increase the blood triglycerides, as has been previously hypothesized (*8*). Regardless of the reason, given the low SUV_{max} obtained in group 1 volunteers, complementary fatty acid loading does not seem necessary to optimize myocardial ^{18}F-FDG signal suppression.

Macrophages contained in atherosclerotic plaques use glucose as fuel and can also metabolize FFAs. The latter requires oxygen to generate adenosine triphosphate, whereas glucose metabolism does not. Because the plaque interior is relatively anaerobic, glucose is the major substrate for macrophages (*24*). Additionally, facilitative transport via the glucose transporter (GLUT) protein system is the pathway predominantly used for ^{18}F-FDG to enter human cells. ^{18}F-FDG uptake in cultured macrophages depends on the degree of macrophage activation (*25*). Macrophage activation increases both GLUT-1 and GLUT-3 expressions, whereas the insulin-sensitive GLUT-4 subtype, which is supposed to be affected by the HFLC diet used in our study, is not detectable.

jnm138594-pm ■ 7/31/14

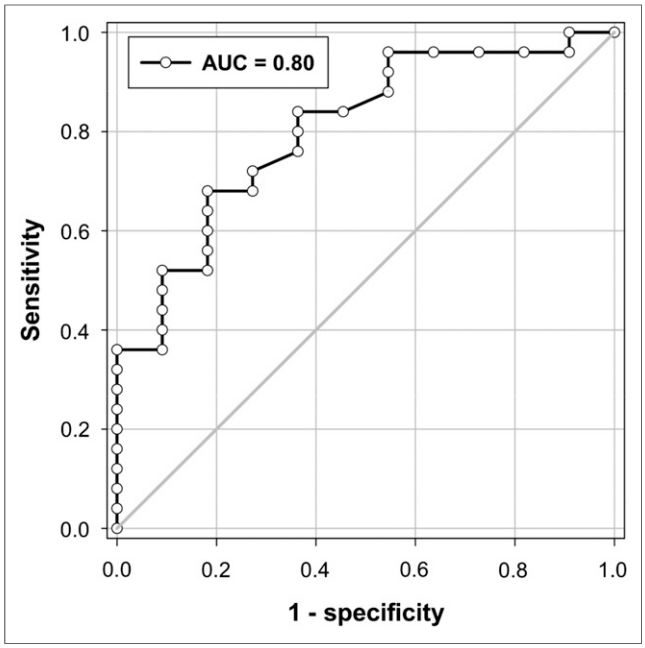

FIGURE 7. Receiver-operating-characteristic curve for cFFA concentration measured at time of ^{18}F-FDG injection for predicting myocardial ^{18}F-FDG uptake suppression (area under the curve [AUC], 0.80).

Therefore, macrophage ^{18}F-FDG uptake should not be influenced by the HFLC preparation.

Cyclic adenosine monophosphate is involved in myocardial glucose uptake through a Ca^{2+}-dependent mechanism, and CCBs reportedly reduce myocardial ^{18}F-FDG uptake in a murine model (*11*). However, our data showed that CCB given 1 h before ^{18}F-FDG injection did not improve myocardial uptake suppression in our volunteers who were asked to fast for 12 h after an HFLC diet. It remains unknown whether CCB could provide a good ^{18}F-FDG uptake suppression in conventionally prepared patients (carbohydrate-permitted diet followed by 6-h fasting). Nevertheless, the low SUV_{max} that we measured in our group 1 volunteers questions the necessity for the use of CCBs, which could potentially lead to side effects. Some authors have attempted to raise cFFA levels by infusing unfractionated heparin to stimulate lipoprotein lipase (*26*). Again, because of the contraindications and the potential side effects of this medication, we think that an HFLC meal followed by 12 h of fasting represents a safer alternative for improving myocardial ^{18}F-FDG uptake suppression.

It is recommended that vascular PET studies involve a longer ^{18}F-FDG circulation time than that for oncology PET imaging. This extended time frame is intended to allow sufficient ^{18}F-FDG accumulation in the arterial wall and to permit the reduction of blood ^{18}F-FDG levels by decay and excretion (*24*). For imaging carotid arteries and aorta, the optimum time point is between 60 and 180 min (*27*). The exact optimum time point for coronary artery imaging is unknown. This time point must account for the risk of a partial-volume effect of ^{18}F-FDG activity spilling into the arterial wall from the vessel lumen and from the myocardium. Our data showed that the decreased myocardial ^{18}F-FDG uptake remained stable over time. It suggests that with adequate myocardial ^{18}F-FDG uptake suppression, the detection of coronary plaque inflammation would not be affected by the myocardial ^{18}F-FDG signal being measured at either 60 or 180 min after ^{18}F-FDG injection. The optimal timing for imaging coronary plaque should predominantly depend on the arterial lesion uptake itself. Further studies are needed to determine the optimal timing for imaging coronary plaques in patients.

Although good myocardial ^{18}F-FDG uptake suppression was obtained in most volunteers prepared with an HFLC diet followed by 12 h of fasting, the myocardial ^{18}F-FDG uptake remained too high in a few volunteers. Therefore, it is extremely important to be able to predict the amplitude of suppression and to thus avoid unnecessary injections of ^{18}F-FDG in inadequately prepared patients. Glucose and insulin levels do not predict myocardial ^{18}F-FDG uptake suppression. One exciting finding of the present work was that myocardial ^{18}F-FDG uptake could be predicted by the total cFFA measured before ^{18}F-FDG injection, with an excellent positive predictive value. The measurement could be easily and quickly (~30 min) obtained in a clinical imaging center and should help to refine the quality of vulnerable coronary plaque detection in patients. Finally, beyond this potential clinical application, our data support the use of our group 1 regimen and the measurement of total cFFA for detecting cardiac involvement of sarcoidosis, which is a definite indication for ^{18}F-FDG PET imaging.

The main limitation of the present work is the relatively small number of volunteers included in the study. However, the study was randomized, and the SUV_{max} obtained in group 1 volunteers was low, compared with the SUV_{max} that we usually obtain in patients referred for oncologic disease. Given the low SUV_{max} obtained in group 1 volunteers, the number of volunteers in the 3 other groups should have been high for identifying difference from group 1. Consequently, we decided to end the study after 9 volunteers because we felt it unethical to continue enrolling volunteers. Healthy volunteers have been recruited to perform this study. That can be seen as another limitation. Nevertheless, our results are in accordance with those obtained in older patients by other groups (*8,10*). Furthermore, it has been previously shown that the myocardial glucose utilization does not increase with age (*28*). Finally, we did not look at regional variability in tracer uptake. Thus, whether any of the interventions increase or decrease regional variability in ^{18}F-FDG uptake remains undetermined as well as the impact of a potential regional uptake on the visualization of coronary plaque inflammation.

CONCLUSION

An HFLC diet administered the evening before ^{18}F-FDG PET/CT followed by fasting for 12 h is a simple and effective method to obtain good myocardial ^{18}F-FDG uptake suppression in a large majority of subjects. No additional benefit was conferred by complementary fatty acid loading or CCB administered 1 h before ^{18}F-FDG injection. Myocardial ^{18}F-FDG uptake is inversely correlated with cFFA levels, which could be used to accurately predict the amplitude of myocardial ^{18}F-FDG uptake suppression. This method could allow avoidance of unnecessary ^{18}F-FDG injection in patients who are not properly prepared. Finally, when adequately suppressed, the myocardial ^{18}F-FDG signal remains low and stable over time, allowing opportunities for coronary inflammation imaging over a broad time range.

DISCLOSURE

The costs of publication of this article were defrayed in part by the payment of page charges. Therefore, and solely to indicate this fact, this article is hereby marked "advertisement" in accordance with 18 USC section 1734. This study was supported by the "Camille and Germaine Damman foundation," Brussels, Belgium. No other potential conflict of interest relevant to this article was reported.

REFERENCES

1. Go AS, Mozaffarian D, Roger VL, et al. Heart disease and stroke statistics: 2013 update—a report from the American Heart Association. *Circulation.* 2013;127: e6–e245.
2. Falk E. Pathogenesis of atherosclerosis. *J Am Coll Cardiol.* 2006;47:C7–C12.
3. Hansson GK. Inflammation, atherosclerosis and coronary artery disease. *N Engl J Med.* 2005;352:1685–1695.
4. Vancraeynest D, Pasquet A, Roelants V, Gerber BL, Vanoverschelde J-L. Imaging the vulnerable plaque. *J Am Coll Cardiol.* 2011;57:1961–1979.
5. Ogawa M, Ishino S, Mukai T, et al. ^{18}F-FDG accumulation in atherosclerotic plaques: immunohistochemical and PET imaging Study. *J Nucl Med.* 2004;45: 1245–1250.
6. Tawakol A, Migrino RQ, Bashian GG, et al. In vivo ^{18}Ffluorodeoxyglucose positron emission tomography imaging provides a non-invasive measure of carotid plaque inflammation in patients. *J Am Coll Cardiol.* 2006;48:1818–1824.
7. Depre C, Vanoverschelde JL-J, Taegtmeyer H. Glucose for the heart. *Circulation.* 1999;99:578–588.
8. Cheng VY, Slomka PJ, Ahlen M, et al. Impact of carbohydrate restriction with and without fatty acid loading on myocardial ^{18}F-FDG uptake during PET: a randomized controlled trial. *J Nucl Cardiol.* 2010;17:286–291.
9. Wykrzykowska J, Lehman S, Williams G, et al. Imaging of inflamed and vulnerable plaque in coronary arteries with ^{18}F-FDG PET/CT in patients with suppression of myocardial uptake using a low-carbohydrate, high-fat preparation. *J Nucl Med.* 2009;50:563–568.
10. Williams G, Kolodny GM. Suppression of myocardial ^{18}F-FDG uptake by preparing patients with a high-fat, low-carbohydrate diet. *AJR.* 2008;190:W151–W156.
11. Gaeta C, Fernández Y, Pavía J, et al. Reduced myocardial ^{18}F-FDG uptake after calcium channel blocker administration: initial observation for a potential new method to improve plaque detection. *Eur J Nucl Med Mol Imaging.* 2011;38:2018–2024.
12. Rogers IS, Nasir K, Figueroa AL, et al. Feasibility of FDG imaging of the coronary arteries: comparison between acute coronary syndrome and stable angina. *JACC Cardiovasc Imaging.* 2010;3:388–397.
13. Cheng VY, Slomka PJ, Le Meunier L, et al. Coronary arterial ^{18}F-FDG uptake by fusion of PET and coronary CT angiography at sites of percutaneous stenting for acute myocardial infarction and stable coronary artery disease. *J Nucl Med.* 2012;53:575–583.
14. Nitta Y, Tahara N, Tahara A, et al. Pioglitazone decreases coronary artery inflammation in impaired glucose tolerance and diabetes mellitus: evaluation by FDG-PET/CT imaging. *JACC Cardiovasc Imaging.* 2013;6:1172–1182.
15. Boellaard R, Hristova I, Ettinger S, et al. EARL FDG-PET/CT accreditation program: Feasibility, overview and results of first 55 successfully accredited sites [abstract]. *J Nucl Med.* 2013;54(suppl 2):498P–499P.
16. International Commission on Radiological Protection (ICRP). Radiation dose to patients from radiopharmaceuticals: addendum 3 to ICRP publication 53. ICRP publication 106. Approved by the Commission in October 2007. *Ann ICRP.* 2008;38:1–197.
17. Gaemperli O, Shalhoub J, Owen DRJ, et al. Imaging intraplaque inflammation in carotid atherosclerosis with ^{11}C-PK11195 positron emission tomography/computed tomography. *Eur Heart J.* 2012;33:1902–1910.
18. Joshi NV, Vesey AT, Williams MC, et al. ^{18}F-fluoride positron emission tomography for identification of ruptured and high-risk coronary atherosclerotic plaques: a prospective clinical trial. *Lancet.* 2014;383:705–713.
19. Tahara N, Kai H, Kakaura H, et al. The prevalence of inflammation in carotid atherosclerosis: analysis with fluorodeoxyglucose-positron emission tomography. *Eur Heart J.* 2007;28:2243–2248.
20. Folco EJ, Sheikine Y, Rocha VZ, et al. Hypoxia but not inflammation augments glucose uptake in human macrophages: implications for imaging atherosclerosis with 18fluorine-labeled 2-deoxy-D-glucose positron emission tomography. *J Am Coll Cardiol.* 2011;58:603–614.
21. Rominger A, Saam T, Wolpers S, et al. ^{18}F-FDG PET/CT indentifies patients at risk for future vascular events in an otherwise asymptomatic cohort with neoplastic disease. *J Nucl Med.* 2009;50:1611–1620.
22. Figueroa AL, Abdelbaky A, Truong QA, et al. Measurement of arterial activity on routine FDG PET/CT images improves prediction of risk of future CV events. *JACC Cardiovasc Imaging.* 2013;6:1250–1259.
23. Coulden R, Chung P, Sonnex E, et al. Suppression of myocardial ^{18}F-FDG uptake with a preparatory "Atkins-style" low-carbohydrate diet. *Eur Radiol.* 2012;22: 2221–2228.
24. Rudd JHF, Narula J, Strauss HW, et al. Imaging atherosclerotic plaque inflammation by fluorodeoxyglucose with positron emission tomography: ready for prime time? *J Am Coll Cardiol.* 2010;55:2527–2535.
25. Deichen JT, Prante O, Gack M, et al. Uptake of (^{18}F)fluorodeoxyglucose in human monocyte-macrophages in vitro. *Eur J Nucl Med Mol Imaging.* 2003; 30:267–273.
26. Ishimaru S, Tsujino I, Takei T, et al. Focal uptake on ^{18}F-fluoro-2-deoxyglucose positron emission tomography images indicates cardiac involvement of sarcoidosis. *Eur Heart J.* 2005;26:1538–1543.
27. Menezes LJ, Kotze CW, Hutton BF, et al. Vascular inflammation imaging with ^{18}F-FDG PET/CT: when to image? *J Nucl Med.* 2009;50:854–857.
28. Kates AM, Herrero P, Dence C, et al. Impact of aging on substrate metabolism by the human heart. *J Am Coll Cardiol.* 2003;41:293–299.